Ridge loads on wind turbine structures

Ken Croasdale, KRCA; Norman Allyn, CMO Consultants Ltd.

Abstract

Wind turbine towers are being planned in ice covered regions subject to pressure ridges (e.g. the Great Lakes). Conical collars are often employed to reduce ice loads from level ice and their associated dynamics. For level ice, downward breaking cones have some advantages. It is not clear if this is the case for pressure ridges. This paper presents an improved method for ridge loads on wind turbines with downward breaking cones and makes comparisons with upward breaking cones.

First year pressure ridges can be formidable ice features and usually control design ice loads in the sub-Arctic. Important components of a ridge creating ice loads are the consolidated layer at the surface (which is considered as solid ice) and the ridge keel below consisting of ice rubble, but much thicker. The load due to the consolidated layer is usually derived as if it is thick level ice. On a cone, methods for level ice assume it can be idealized as a plate on an elastic foundation (the water) and equations have been developed for upward and downward breaking cones. But for a ridge on a downward cone, to break the consolidated layer downwards requires it to be pushed into the keel rubble below. This will have a different foundation modulus than water buoyancy. A method is developed to account for this difference. The method uses an iterative approach to determine the point of breaking of the consolidated layer (and associated load) accounting for the ridge geometry, keel rubble shear strength, the flexural strength of the consolidated layer and the buoyancy forces. The keel loads on the vertical shaft below the conical collar are based on the method currently in ISO 19906 (2010) but modified to add the effect of additional rubble in the keel from breaking the consolidated layer downwards.

In examples, it is shown that the breaking force can be about twice that of breaking the consolidated layer without the keel present. This might be seen as a disadvantage for downward breaking cones vs upward breaking. However, it is also shown that the clearing forces on an upward cone are higher; which tends to balance out the lower breaking force. Example loads are given on typical wind turbine bases due to typical ridges. Upward and downward breaking configurations are compared.

The paper provides new methods for ice loads due to ridges acting on wind turbine structures not currently covered by existing methods.

Offshore wind turbine structures overview

For aerodynamic reasons, wind turbine towers need to be as slender as possible. This can present structural engineering challenges, especially in the context of cyclic loads which may create vibrations, with resulting dynamic magnification and fatigue damage. These issues can become more challenging as turbines increase in size.

In the conventional offshore (with no ice) the slender turbine shaft is usually carried down through the water line to the sea floor foundation in order to minimize the wave loads. In current wind turbine practice the relevant codes (e.g. DNV-OS-J101, 2014; IEC 61400-3, 2009) devote considerable content to how wave loads are specified and combined with the wind turbine loads. The structure and foundation are designed for the maximum quasi-static combined loads, dynamic responses and fatigue.

The codes also require the same general approach to be used in ice covered regions. In general, ice loads will be higher than wave loads, so the design of wind turbines in ice areas can present a greater challenge. The cyclic nature of ice loads can be critical because the frequencies of ice load cycles can be closer to structure natural frequencies. This is particularly the case for vertical cylindrical shapes against which the ice crushes. In ice engineering there are many case histories of structures in ice areas being subject to severe vibrations and sometimes failure due to dynamic magnification of the ice loads.

Experience with slender light piers in the Baltic led to studies of the phenomenon (e.g. Karna and Turunen 1989). It was also found that ice load frequencies could be lowered and moved away from the natural periods of the structure by fitting conical collars. A conical shape at the ice line changes the ice failure mode from crushing to bending. This has the advantage of lower global ice loads as well as lowering the cyclic frequencies. For these reasons, sloping faces, despite their additional complexity, are often used for structures in ice.

To date there have been only a few wind turbines placed in areas subject to ice and all have conical shapes at the water line, as do those currently being designed. Most conical structures use an upward breaking cone but downward breaking can also be incorporated. Downward breaking has the advantage of lower clearing loads and is of course used extensively by ice breaking vessels. Downward breaking is used less extensively for fixed structures because it can create a less robust and more complex structure. However the slender shafts of wind turbines lend themselves to either upward or downward breaking conical collars. Operationally, downward cones have the advantage of better vessel access and a platform for landing maintenance personnel and equipment.

The challenge for the ice engineer to be able to specify ice loads for both upward and downward cones for the relevant ice regime. In shallow water, turbines are subject to level ice which is landfast for most of the ice season and free of significant ice ridges. As turbines are placed further from shore the ice is more mobile and contains ice pressure ridges which can generate high ice loads. To date there are no precedents for calculating ice pressure ridge loads on downward breaking configurations. The work described in this paper addresses this deficiency.

Idealization of first year pressure ridges for load calculations

First it is appropriate to define the morphology of first year pressure ridges and how they are usually idealized for load calculations. Considerable work has been done on surveying ridges to understand their shapes and internal structures (e.g. Timco et al 2000, Suddom et al 2011). Ridges are formed when two ice sheets fail against each other in areas of pressured ice. Out of plane failures in bending and buckling modes lead to the creation of ice rubble which builds upwards and downwards creating a ridge with 90% of its volume below the water. This leads to a ridge with a large keel of ice rubble and a small sail. At the water line, the rubble consolidates by freezing. The resulting ridge is usually idealized as shown in **Fig.1**.

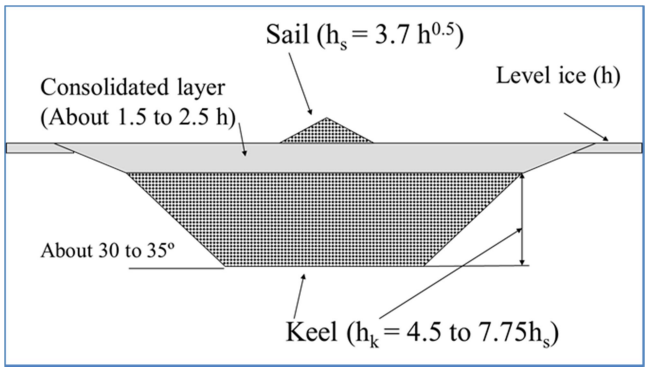

Fig. 1: Idealized geometry of a first year pressure ridge (Palmer and Croasdale 2013).

Methods for ice loads due to such a ridge are discussed in ISO 19906 (2010) and other references (Palmer and Croasdale 2013). On vertical faces the methods treat the consolidated layer (CL) as solid ice and suggest the equations for level ice in crushing be used for that component. The keel is usually treated as a granular material with cohesion and friction and methods similar to those used in soil mechanics are suggested to calculate the keel load (e.g. Dolgopolov et al 1985). The two components of load are then added.

ISO 19906 is silent on how to calculate first-year ridge loads on sloping structures but generally implies the same approach with the CL being treated as level ice; in this case failing in bending. The keel load then being calculated using an adaptation of Dolgopolov et al (1985). Other methods for generic sloping structures are reviewed by Croasdale et al (2012a and 2018).

Conical collars, as might be used on wind turbines are a special case because they can be configured for the consolidated layer to fail in bending on the collar and for the ridge keel to fail on the vertical shaft below. This is illustrated conceptually in **Fig. 2.**

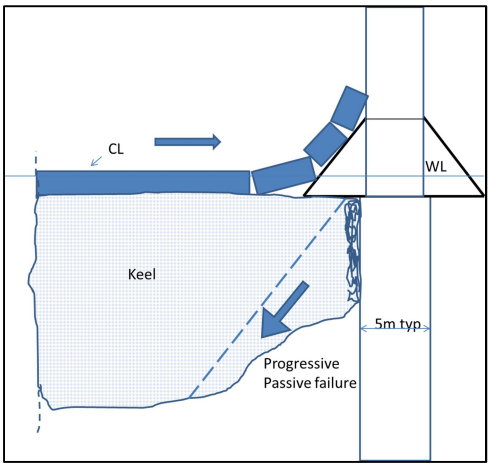

Fig. 2 - Ridge failure on an upward breaking conical collar with vertical shaft below

Ice load methods for level ice

To start, the methods for level ice loads on conical collars will be reviewed. This is because; first, most of the ice cover is level ice; second, its motion creates cyclic loads which have to be part of the dynamic analysis of the structure (although this is not the focus of this paper); third, the methods for level ice can be adapted for the CL of a ridge. Methods for upward breaking are first discussed

Upward breaking of level ice on conical collars

In ISO 19906 (2010) two methodologies are given for level ice loads on sloping structures. These can be used for conical collars. Method 1 is based on Ralston (1980) and Method 2 on Croasdale et al (1994); the latter method was recently updated (Croasdale et al, 2016) and will be in the new version of ISO 19906 and is the one described here. The overall approach is shown in **Fig. 3**.

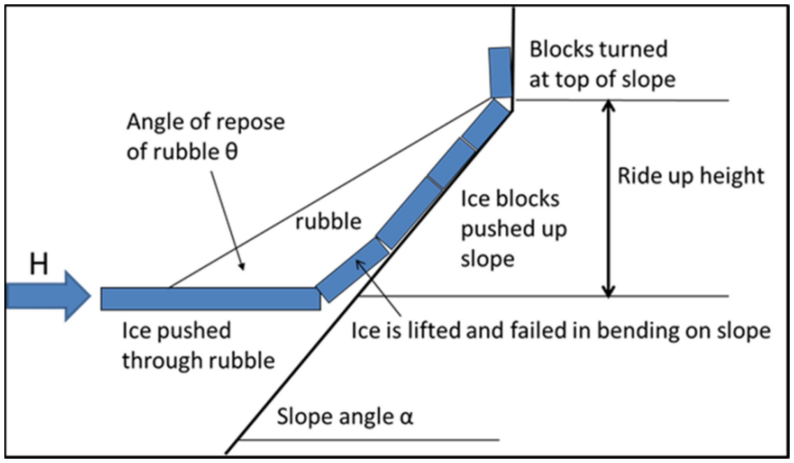

Fig. 3- Load components for level ice acting on a conical (sloping) structure (After Croasdale et al 1994, 2016)

The overall equation for the horizontal ice load (H) is,

$$H = [H_B + H_R + H_P + H_L + H_T]I_p \quad (1)$$

Where, H_B is the horizontal component of the force to break the ice; H_R is the horizontal component of the force to push the broken ice blocks up the slope; H_P is the force to push the oncoming ice through any ice rubble on top of the ice sheet; H_L is the horizontal component of the force required to lift the ice rubble prior to breaking of the ice sheet; H_T is the horizontal component of the force to turn the ice blocks at the top of the slope as they meet the vertical shaft. Ip is the correction for the effect of in-plane compression in the ice sheet due to H. This increases the effective flexural strength.

Detailed equations for the various load components are not given here but they are given in the paper presented at the last ATC (Croasdale et al 2016) and will be in the updated ISO 19906.

Loads for a typical turbine base as might be used in the Great Lakes of North America are given in Table 1. These loads are for an upward cone based on a design with a conical collar on 5m diameter shaft. A level ice thickness of 0.6m is used, this being the estimated 50 year value as specified by the turbine codes (for Lake Erie). Other input parameters are shown in the table. A sensitivity is performed on cone angle. For 60 degrees (the steepest), the horizontal load is estimated at 1.34MN; this is for flexural strength of 500kPa which is deemed appropriate for fresh water ice (a lower value would be used for sea ice). It can be seen that as the cone angle is made shallower the horizontal load is reduced although there is not much advantage in going shallower than about 50 degrees because for a given shaft diameter, the water line width also increases which increases clearing loads. For an assumed rubble repose angle (θ in Fig. 3) of 15 degrees (based on observations at Confederation Bridge (Croasdale et al 2016), it can be seen that the ride up and clearing loads (HR, HP, HL, HT) make up slightly more than half the total load (0.74MN out of a total of 1.34MN for the 60 degree cone). This proportion is actually higher for shallower cones.

Table 1: Typical loads due to 0.6m thick level ice acting on an upward conical collar on a 5m dia. turbine base

		Upward breaking cone		
Input Data in blue: Derived values in black and results in green		**0.6m (15 degrees of rubble) 60° cone**	**0.6m (15 degrees of rubble) 50° cone**	**0.6m (15 degrees of rubble) 45° cone**
Flexural strength of ice	(kPa)	**500**	**500**	**500**
Specific weight of ice	(kN/m^3)	**8.83**	**8.83**	**8.83**
Slope Angle	(deg)	**60**	**50**	**45**
Rubble angle of repose	(deg)	**45**	**35**	**30**
Waterline width (D)	(m)	**7.5**	**8.6**	**9.3**
Shaft dia. Width for HT	(m)	**5**	**5**	**5**
Width for centre ride up	(m)	6.25	6.8	7.15
Slope height (hs)	(m)	**2.2**	**2.2**	**2.2**
Ice-cone friction		**0.1**	**0.1**	**0.1**
Ice-ice friction		**0.25**	**0.25**	**0.25**
Thickness for ride up	(m)	**0.6**	**0.60**	**0.60**
Thickness for breaking (hb)	(m)	**0.6**	**0.60**	**0.60**
Rubble porosity		**0.15**	**0.15**	**0.15**
Cohesion of rubble	(kPa)	**5**	**5**	**5**
wB	(m)	21.61	21.61	21.61
Ride up or ride down height (m)		4.00	4.00	4.00
Predicted Horizontal Load (MN)		**1.34**	**1.09**	**1.08**
HB2		0.60	0.41	0.36
HP		0.02	0.03	0.043
HR		0.38	0.33	0.332
HT		0.02	0.04	0.044
HL		0.32	0.29	0.307
Total Horizontal Load(MN)		1.34	1.09	1.084
Vertical Load (MN)		0.60	0.73	0.86

Downward breaking of level ice on conical collars

The physics of downward breaking are the same except that buoyant forces replace gravity forces. This leads to lower clearing and ride down forces, because buoyant forces (weight of ice in water) are about 10% of gravity forces (weight of ice in air).

Load comparisons up vs down

Load comparisons for the same turbine base with the same inputs are shown in Table 2.The main point is that the clearing forces are significantly reduced so that the total loads are also lower. For a 60 degree cone, the total load is reduced from 1.34MN to 0.65MN; a useful reduction. Will the same reduction in load be the case for pressure ridge interaction? This is addressed next.

Table 2: Typical loads due to 0.6m thick ice acting on a downward conical collar on a 5m dia. shaft turbine base

		Upward breaking cone			Downward breaking cone		
Input Data in blue: Derived values in black and results in green		0.6m (15 degrees of rubble) 60° cone	0.6m (15 degrees of rubble) 50° cone	0.6m (15 degrees of rubble) 45° cone	0.6m (15 degrees of rubble) 60° cone	0.6m (15 degrees of rubble) 50° cone	0.6m (15 degrees of rubble) 45° cone
Flexural strength of ice	(kPa)	500	500	500	500	500	500
Specific weight of ice	(kN/m^3)	8.83	8.83	8.83	8.83	8.83	8.83
Slope Angle	(deg)	60	50	45	60	50	45
Rubble angle of repose	(deg)	45	35	30	45	35	30
Waterline width (D)	(m)	7.5	8.6	9.3	8.5	10.1	11.1
Shaft dia. Width for HT	(m)	5	5	5	5	5	5
Width for centre ride up	(m)	6.25	6.8	7.15	6.75	7.55	8.05
Slope height (hs)	(m)	2.2	2.2	2.2	3.0	3.0	3.0
Ice-cone friction		0.1	0.1	0.1	0.1	0.1	0.1
Ice-ice friction		0.25	0.25	0.25	0.15	0.15	0.15
Thickness for ride up	(m)	0.6	0.60	0.60	0.60	0.60	0.60
Thickness for breaking (hb)	(m)	0.6	0.60	0.60	0.60	0.60	0.60
Rubble porosity		0.15	0.15	0.15	0.15	0.15	0.15
Cohesion of rubble	(kPa)	5	5	5	5	5	5
wB	(m)	21.61	21.61	21.61	21.61	21.61	21.61
Ride up or ride down height (m)		4.00	4.00	4.00	4.80	4.80	4.80
Predicted Horizontal Load (MN)		**1.34**	**1.09**	**1.08**	**0.65**	**0.50**	**0.46**
HB2		0.60	0.41	0.36	0.53	0.39	0.35
HP		0.02	0.03	0.043	0.002	0.004	0.005
HR		0.38	0.33	0.332	0.054	0.048	0.048
HT		0.02	0.04	0.044	0.003	0.004	0.005
HL		0.32	0.29	0.307	0.053	0.051	0.056
Total Horizontal Load(MN)		1.34	1.09	1.084	0.647	0.497	0.464
Vertical Load (MN)		0.60	0.73	0.86	0.29	0.34	0.38

Ice load methods for ridges

Ridges acting on an upward breaking cone

Overall approach

As already indicated in **Fig. 2**, the general approach for ridge forces on a conical collar is to design the structure such that the CL of the ridge acts on the cone and the keel acts on the vertical shaft below. The approach is then to calculate the load due to the CL acting on the cone as though it was a thicker level ice sheet and calculate the keel load as though it was acting on the vertical structure below it. The two loads are added. This is an idealization because water level variation usually require some of the keel to also act on the collar at the higher water levels, however the average structure width for the keel action is approximately the lower shaft width.

CL Loads

For upward breaking, the method just described for level ice will be used as it is hypothesized that the load to separate the two parts of the ridge can be ignored because the tensile strength of ice rubble is known to be very low and the CL will separate from the keel at low loads (Palmer and Croasdale 2013). This is an approximation but seems to be supported by load measurements at Confederation Bridge which also has a similar geometry (see accompanying paper at this conference, Croasdale et al 2018; also Brown et al 2010).

With this assumption the "level ice" calculation can be repeated with the thickness of CL (h_{CL}). The 50 year value for CL thickness has been derived at 1.1m for a typical Lake Erie location. Its strength will be lower than level ice due to the generally higher porosity in a ridge, so a value of 350kPa is used for flexural strength. Other inputs with

sensitivities are given in Table 3. The load is in the range of 2.8 to 3.7MN and the breaking components (HB) about 30 - 40% of the total (with a range 1.1 to 1.4MN).

Table 3: Range of CL loads for an upward 60 degrees conical collar

Input Data in blue: Derived values in black and results in green		**60 degree CL 1.1m; friction = 0.1**	**60 degree CL 1.1m; friction = 0.15**	**More rubble**
Flexural strength of ice	(kPa)	**350**	**350**	**350**
Specific weight of ice	(kN/m^3)	**8.83**	**8.83**	**8.83**
Slope Angle	(deg)	**60**	**60**	**60**
Rubble angle of repose	(deg)	**45**	**45**	**35**
Waterline width (D)	(m)	**7.5**	**7.5**	**7.5**
Slope height (hs)	(m)	**2.50**	**2.50**	**2.50**
Width for HT (Dt)	(m)	**5**	**5.00**	**5.00**
Width for centre ride up	(m)	**6.25**	**6.25**	**6.25**
Ice-cone friction		**0.1**	**0.15**	**0.1**
Ice-ice friction		**0.25**	**0.25**	**0.25**
Thickness for ride up	(m)	**1.1**	**1.1**	**1.1**
Thickness for breaking (hb)	(m)	**1.1**	**1.1**	**1.1**
Rubble porosity		**0.15**	**0.15**	**0.15**
Cohesion of rubble	(kPa)	**5**	**5**	**5**
wB	(m)	34.05	34.05	36.59
Ride up height	(m)	**5.80**	**5.80**	**5.80**
Results				
Predicted Horizontal Load (MN)		**2.78**	**3.30**	**3.77**
HB		1.10	1.38	1.21
HP		0.04	0.04	0.120
HR		0.98	1.14	1.016
HT		0.07	0.07	0.075
HL		0.58	0.66	1.350
Total (MN)		2.78	3.30	3.767

Keel loads

As already indicated in **Fig. 2**, the keel is essentially acting on a vertical shaft. A solution to this problem was developed by Dolgopolov et al (1975) and is incorporated into ISO 19906 (2010). The solution given is for a downward passive failure of the ridge keel as shown in the left side of **Fig. 4**. A refinement is to recognize that as the structure penetrates the keel, it may also induce the horizontal plug failure shown on the right in Figure 4. The lowest of the two will control.

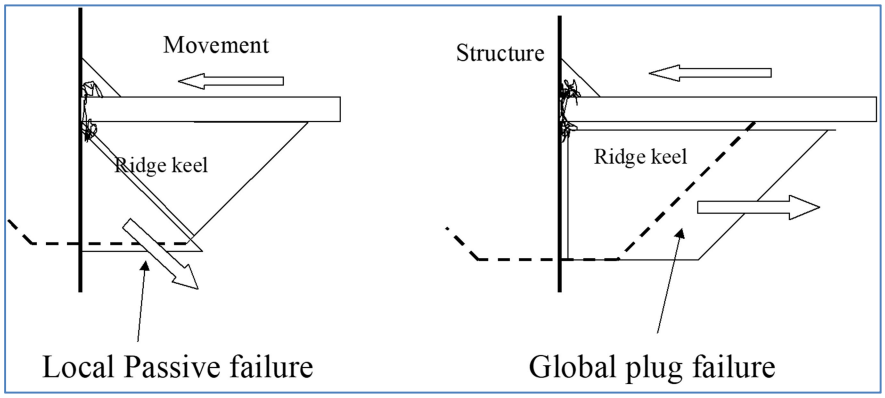

Fig. 4- Two bounding keel failure modes on a vertical structure

One analytical approach proceeds by stepping through the ridge and determining the two loads (passive shear and shear plug) at each increment. The actual keel load at each increment is the lower of the two. If the two curves cross, prior to penetration to the deepest part of the keel (including any surcharge) then this is the controlling load. Keel loads from narrow ridges will often be controlled by the plug failure. It is therefore useful to include it in a probabilistic model, but may not control in deterministic calculations when the widest ridge will be chosen.

The algorithm for the passive local failure of rubble in the keel is given in ISO 19906 (2010) as,

$$F_{pa} = K_p h_k D\left(\frac{h_k K_p \gamma_e}{2} + 2c\right)\left(1 + \frac{h_k}{6D}\right) \quad (2)$$

where D is the structure width, h_k is the keel thickness c is the cohesion in the keel, K_p is the passive pressure coefficient of the material ($\approx \tan[45° + \varphi/2]$), φ is the internal friction angle and γ_e is the buoyant unit weight of the keel rubble (accounting for keel porosity), given by,

$$\gamma_e = (1-e)(\rho_w - \rho_i)g \quad (3)$$

where e is the porosity of the keel rubble, ρ_w is the density of water, ρ_i is the density of ice.

Although not in ISO, Dolgopolov et al (1975) recommended that the keel depth be increased by a surcharge factor (s) to account for the surcharge created at the bottom of the keel due to non-clearing rubble; that is,

$$h_k = h_{ko} + sD \quad (4)$$

where, h_{ko} is the original keel depth and D is the structure width. The value of s can be as high as 0.5; in fact Dolgopolov et al (1975) recommended this as an upper value. For wide structures, we recommend the surcharge factor be limited to about 0.05 – 0.1. For narrow structures, as in the case of the turbine bases (5m), it will be seen that later we use 0.5 for upward cones and a value up to 0.75 for downward cones. This is to account for material from the CL being pushed down for a downward cone – as will be discussed. Model tests may be useful in determining surcharge factors for various widths and shapes.

Another key issue is whether friction and cohesion should be combined. There is significant evidence that they should not be. The nature of ice rubble is that cohesion is created by the freeze bonding and sintering between the

ice blocks. Once broken, the evidence suggests that it is not re-established during the time of typical interaction. After the bonds are broken, the ice rubble will have a residual friction but this should not be combined with cohesion. Checks should be made assuming first pure cohesion then a residual friction. Many sample calculations indicate that if the appropriate values are chosen for cohesion, the residual friction load will not control. Nevertheless, it is sometimes useful to compare a purely frictional model with a purely cohesive model. In some situations, cohesion and friction may be combined if these values have been interpreted from rubble strength tests as a combination.

Another issue is that because of the trapezoidal shape of a ridge, penetration is gradual and when the interaction is nominally controlled by the maximum ridge thickness, the area of the "side shears" has been reduced from their theoretical triangular maximums. It will be shown that the version of Dolgopolov with the largest "shape factor" is based on full triangular side shears which cannot occur with gradual penetration (because the material subject to the full triangular side shears has already been failed). A modified version has been derived which assigns only residual friction to the side shears.

The issue of surcharge also needs to be accounted for in context. If the Dolgopolov equation is used with cohesion, it will be erroneous to simply use the surcharge factor (s) to increase effective thickness as defined by equation (4). This is because the ice creating the surcharge has already been sheared and has no cohesion. A more accurate approach has been developed and is given in the equation below.

$$F = 2cDh_k[1+2h_i/D] + 0.5Dh_k^2\gamma K_p^2[1+2h_i/D] + 0.5D\gamma[h_k s]^2 + h_k^2\gamma \tan\Phi_R\,[0.5h_k+sD+s^2(h_k+0.5D)] \quad (6)$$

The above equation includes both cohesion and frictional shearing but as discussed above, it is not recommended that they normally be combined. However, to retain both is useful because some researchers still interpret the peak loads in rubble shear tests in various ways, a) pure cohesion; b) pure friction; c) a combination of the two. The equation contains a residual friction term ($\tan\Phi_R$) associated with the side shears and surcharge build-up. Clearing is based on both buoyancy and friction. The original keel thickness is used for shearing the unbroken keel frontal failure plane but the side shears are assumed to be sheared incrementally in thin strips of width hi (level ice thickness (hi) being a proxy for block size). Surcharge (s) is added to the clearing of the debris created by keel shearing.

Keel load

A spreadsheet using **Eq. 6** is used. As shown in **Fig. 5**, this spreadsheet also shows other formulations but the one labelled "Prediction" is that of **Eq. 6**.This is slightly higher than the current ISO method because of the surcharge. The plug load never gets as low as the passive failure loads so does not control. The results using the keel depths for a ridge forming early in the winter season (16 m), and average (top) cohesion strength (12kPa), and a residual friction of 30 degrees are shown in Figure 5. The shaft diameter has been increased to 5.5m to recognize the effect of the cone on the effective shaft diameter (some of the keel at high water level acts on the cone). The predicted keel load for a 5 m bottom ridge width is 4.58MN. Not shown, but for a 30 m bottom width, the load does not change, because the shear plug load is not controlling and will only increase with increased bottom width.

It should be noted that a surcharge factor of 0.5 has been applied, which is often unaccounted for, but was recommended by the originators of the keel load models (Dolgopolov et al, 1975); (and can be seen in model tests)

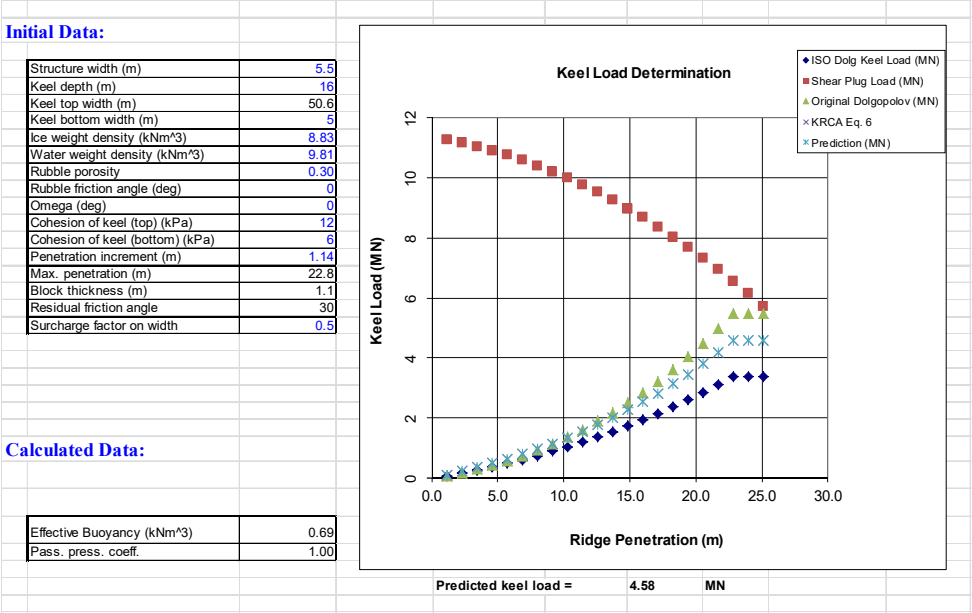

Fig. 5- Ridge keel load; Calculation for cohesion strength 12kPa (top), and a residual friction of 30 degrees.

Example total loads

For an upward breaking collar we can now add this keel load of 4.58MN to the upward breaking load of the consolidated layer of 3.3MN for a total ridge load of 7.9MN. Clearly for global load design the pressure ridge with a load of 7.9MN will control over the "level ice load" calculated earlier of 1.34MN.

Ridge interaction with a downward breaking conical collar

Overall approach

This is the same, calculating the force to fail the CL which is then added to the keel load.

Downward failure of the (CL) consolidated layer

However, the downward breaking of the CL is different from downward breaking of level ice (covered earlier in the paper) because the underlying keel adds additional resistance which has to be overcome before flexural failure can occur. It's a complex problem because the state of the keel (whether it has already been sheared by the shaft) is uncertain. We could use the same model as for level ice without a keel below it, but it will be a lower bound (non-conservative).

A more realistic (but still bounding) approach to the problem is given in the following. First we examine the initial penetration when the ridge keel has not yet been fully penetrated. This is shown in **Fig. 6**. It is the vertical force V generated at the cone which eventually breaks the CL, but it also has to overcome the shearing of keel below as well buoyancy of the keel and CL as they are pushed down. These components are shown in **Figs. 6 and 7**.

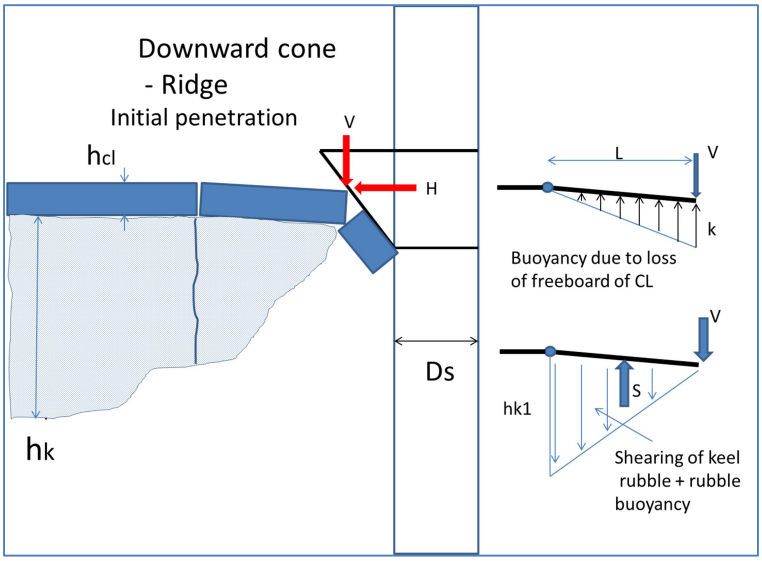

Fig. 6: Initial penetration into ridge: CL is broken downwards but has to overcome resistance of keel below it

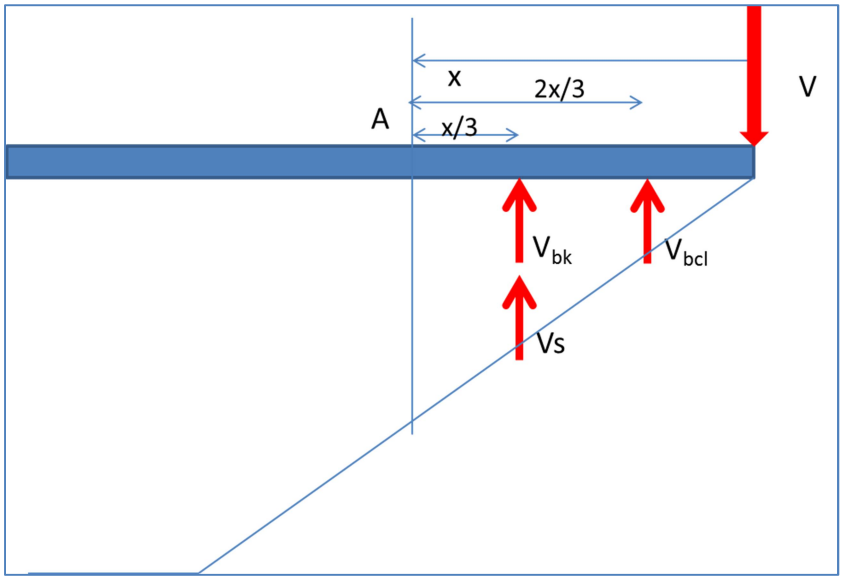

Fig. 7 - Scheme to calculate bending moment at A

The scheme to calculate the breaking load is shown in **Fig. 7**.

First the bending moment at A, a distance x from the end, is computed:

$$M_A = Vx - x(V_{bk} + Vs)/3 - 2xV_{bcl}/3 \qquad (7)$$

Where, V is the total force V applied by the cone, x is the distance to the break, Vbk is the vertical force to overcome the buoyancy of the keel, Vs is the force to shear the keel rubble and Vbcl is the force to overcome the buoyancy of the CL as it is pushed down.

Now consider the cross section of the CL at A, it is w_b wide and h_{cl} thick. If the induced flexural failure stress is σ, then by Engineer's theory of bending:

$$M/I = \sigma/y \quad (8)$$

$$I = w_b h_{cl}^3/12 \text{ and } y = h_{cl}/2, \text{ so} \quad (9)$$

$$M = w_b h_{cl}^2 \sigma/6 \quad (10)$$

Substituting:

$$w_b h_{cl}^2 \sigma/6 = Vx - x(V_{bk} + Vs)/3 - 2xV_{bcl}/3 \quad (11)$$

Solve for V which is the force to create the failure stress, σ:

$$V = w_b h_{cl}^2 \sigma/6x + (V_{bk} + Vs)/3 + 2V_{bcl}/3 \quad (12)$$

Also: $$V_{bcl} = w_b y \rho_w 0.33x \quad (13)$$

$$Vs = 0.33cx\tan30(w_b+x) \quad (14)$$

$$V_{bk} = 0.33(0.5)\,\gamma x^2 w_b \tan30 \quad (15)$$

These components can be calculated as a function of x giving the load required to fail the CL as a function of x. The lowest load is the governing load and the value of x is where the crack occurs.

Before proceeding with an example, the issue of w_b deserves some more attention and a scheme is needed to go from 2D to 3D. The theory developed for a level ice sheet failing in bending uses beam on an elastic foundation theory with a correction for 3D breaking by using the length of the circumferential crack as the effective beam width (see Croasdale et al 1994 and 2016). **Fig. 8** shows the transformation. In the figure, R is the distance to the failure crack. Beam on elastic foundation theory gives:

$$R = \pi Lc/4 \quad (16)$$

Where:

$$L_c = \left(\frac{Eh^3}{12\rho_w g(1-\nu^2)}\right)^{1/4} \quad (17)$$

It can be seen from **Fig. 8** that the length of the circumferential crack in this situation is:

$$w_b = \pi R = \pi^2 Lc/4 \quad (18)$$

The broken channel width is 2R. If 2R is less than D the structure width, then the expression for w_b has to recognize this situation. The arrangement shown in **Fig. 9** is assumed. This is shown for a flat structure in order to bound the problem and should be slightly conservative. In this case the actual w_b is given by:

$$w_b = D + \pi^2 Lc/4 \quad (19)$$

Lc is a function of the foundation modulus, which for a floating ice beam or plate is proportional to the buoyancy (which is proportional to $\rho_w g$). The effect of the increased stiffness due to the keel below the CL will be to reduce Lc and hence w_b. An approximate adjustment to w_b will be:

$$w_{bk} = w_{bi}\,[(V_{bcl} + V_s + V_{bk})/V_{bcl}]^{0.25} \quad (20)$$

With this adjusted w_b (w_{bk}) the actual value of R (distance to crack) is given by:

$$R_k = w_{bk}/\pi \quad (21)$$

This is the value of x at which failure of the CL will occur. But note that if $2R_k$ is less that D then the actual w_b to be used in the calculations is:

$$w_b = D + w_{bk} \quad (22)$$

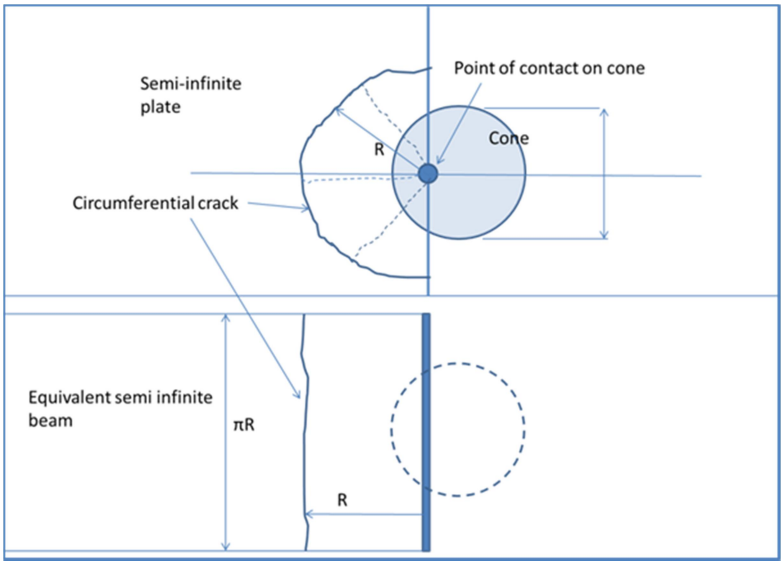

Fig. 8: Transposing the circumferential crack length to a beam of width πR

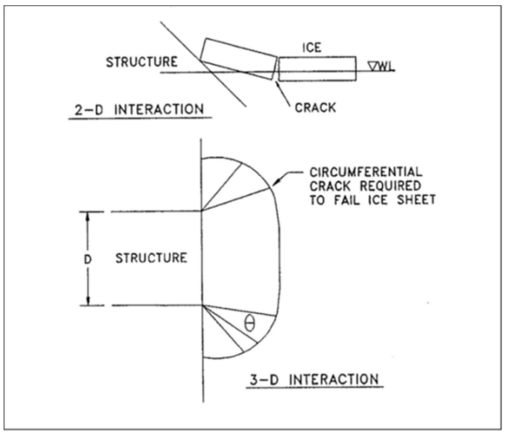

From Croasdale et al, 1994

Fig. 9 - Situation if structural width is greater than 2R (Circumferential crack length is increased by structure width)

The calculation is conducted by iteration because it is difficult to solve in closed form, and an example is given in Table 3. The top seven rows are inputs. The controlling load is with a value of x matching R, this is highlighted in yellow. The value of H to break the CL is 1.04MN. In this case the broken width is greater than the structure width, so the second version of the calculation with D added to w_{bk} is not needed.

Table 3: Initial penetration into ridge with a keel slope of 30 degrees.

		ρw	9.81	kN/m3	σ	350	kPa	α	60	deg
		ρi	8.83	kN/m3	θ	30	degrees	μ	0.15	
		porosity	0.25		γ	0.11	m	ξ	2.54	
		γ	0.735	kN/m3	wbi	36.95	m	D	8.5	m
		c	12	kPa	hcl	1.1	m			
		hk	16	m	ϕ	25	degrees			
		E	4	GPa	Lc	14.97	m			
									Broken	
x (m)	Vbcl (MN)	Vs (MN)	Vbk (MN)	Relative k	wbk	R(m)	V (MN)	H (MN)	width (m)	>D?
1	0.013159	0.086762	0.002587	7.790	22.12	7.04	1.5995	4.07	14.08	Y
2	0.015753	0.110274	0.006194	8.393	21.71	6.91	0.8296	2.11	13.82	Y
3	0.023193	0.169467	0.013679	8.897	21.40	6.81	0.5868	1.49	13.62	Y
4	0.030477	0.232231	0.023968	9.406	21.10	6.72	0.4825	1.23	13.43	Y
5	0.037569	0.298337	0.036931	9.924	20.82	6.63	0.4337	1.10	13.25	Y
6	0.044483	0.36787	0.052474	10.450	20.55	6.54	0.4134	1.05	13.08	Y
6.5	0.047572	0.401991	0.060794	10.728	20.42	6.50	0.4078	1.04	13.00	Y
7	0.051232	0.440915	0.070507	10.983	20.30	6.46	0.4103	1.04	12.92	Y
8	0.057827	0.517546	0.090953	11.523	20.06	6.38	0.4186	1.06	12.77	Y
9	0.064279	0.59783	0.113738	12.070	19.82	6.31	0.4352	1.11	12.62	Y
10	0.070597	0.681829	0.138798	12.624	19.60	6.24	0.4580	1.16	12.48	Y

The mature situation with complete penetration into the keel is now reviewed. **Fig. 10** endeavours to show the mature situation when the ridge has been penetrated to its maximum thickness and when the highest loads will be generated.

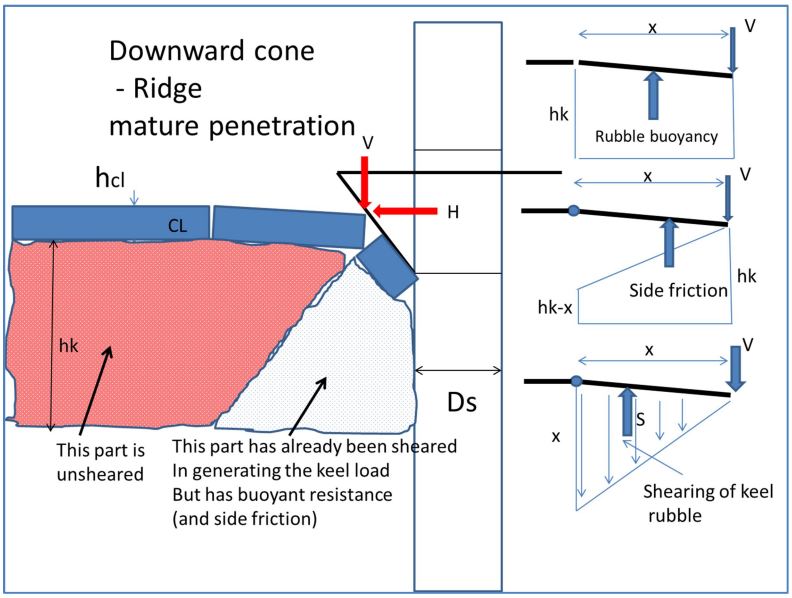

Fig. 10: Breaking of the CL with full keel depth below the CL

Again, the method looks at the breaking of the next ice piece which is given an unknown length value of x. The equations for the various components are now:

$V_{bcl} = by\rho_w 0.33x$ (unchanged) (23)

$Vs = 0.33cx\tan 45(w_b+x)$ (prior shear plane assumed at 45º) (24)

$F_{bk} = \gamma x h_{k1} b$ (25)

$V_{bk} = 0.5\ \gamma x h_{k1} b$ (26)

A new term is side friction of the plug of failed material (V_{SS}):

$V_{SS} = 0.5\gamma h_k x\ (2h_k - x)\tan\varphi$ (27)

$V = w_b h_{cl}^2 \sigma/6x + 0.5V_{bk} + Vs/3 + 2V_{bcl}/3 + 2V_{ss}/3$ (28)

Results for a typical example are shown in Table 4.

Table 4: Mature penetration; Loads to fail the CL in downward breaking

ρw	9.81	kN/m3	σ	350	kPa	α	60	deg
ρi	8.83	kN/m3	θ	30	degrees	μ	0.15	
porosity	0.25		y	0.11	m	ξ	2.54	
γ	0.735	kN/m3	wbi	36.95	m	D	8.5	m
c	12	kPa	hcl	1.1	m			
hk	16	m	ϕ	25	degrees			
E	4	GPa	Lc	14.97	m			

x (m)	Vbcl (MN)	Vs (MN)	Vbk (MN)	VSS (MN)	Relative k	wbk	R (m)	V (MN)	H (MN)	Broken width (m)	>D ?	new σ	New V	New H	Ratio
1	0.013	0.150	0.217	0.085	35.39	15.15	4.82	1.293	3.29	9.64	y	547.28	1.896	4.82	1.47
2	0.011	0.136	0.178	0.164	30.10	15.78	5.02	0.808	2.05	10.04	y	468.38	0.996	2.53	1.23
3	0.017	0.223	0.278	0.239	30.75	15.69	4.99	0.753	1.91	9.99	y	460.90	0.870	2.21	1.16
4	0.022	0.312	0.369	0.307	31.47	15.60	4.97	0.783	1.99	9.93	y	466.05	0.875	2.22	1.12
4.94	0.027	0.402	0.453	0.366	32.15	15.52	4.94	0.845	2.15	9.88	y	475.82	0.925	2.35	1.09
5	0.028	0.408	0.459	0.370	32.20	15.51	4.94	0.850	2.16	9.87	y	476.56	0.929	2.36	1.09
6	0.033	0.511	0.547	0.428	32.93	15.43	4.91	0.933	2.37	9.82	y	489.71	1.005	2.55	1.08
7	0.038	0.622	0.635	0.480	33.68	15.34	4.88	1.024	2.60	9.76	y	504.35	1.093	2.78	1.07
8	0.044	0.739	0.722	0.526	34.43	15.25	4.86	1.121	2.85	9.71	y	519.88	1.187	3.02	1.06

The controlling load is 2.35MN. This table shows an additional iteration to account for the compression in the ice sheet increasing the effective flexural strength (see the last three columns). This correction is also in the methodology for the upward cone and is included to be consistent between upward and downward loads. In this case it can be seen that the broken width is still greater than the value of D of 8.5m used in the input.

Example total loads

As noted, the CL failure load is calculated at 2.35MN. This compares to the range of breaking loads for the upward cone of 1.1 to 1.4MN (see Table 3). The upward cone however is penalised further because of the ride up and turning forces which are in air so are higher than in water, giving the total CL load for the upward cone of 3.3MN. If we added the same ride down and clearing loads for the downward cone, but factored for their weight in water, the total load would be about 2.7MN. This is not considered the best approach; rather assume the CL debris is added to the keel clearing load by using a greater surcharge factor. With this assumption (s = 0.75), the accompanying keel load is shown in Figure 11. The predicted keel load is 5.46MN. So the total ridge load is 7.81MN.

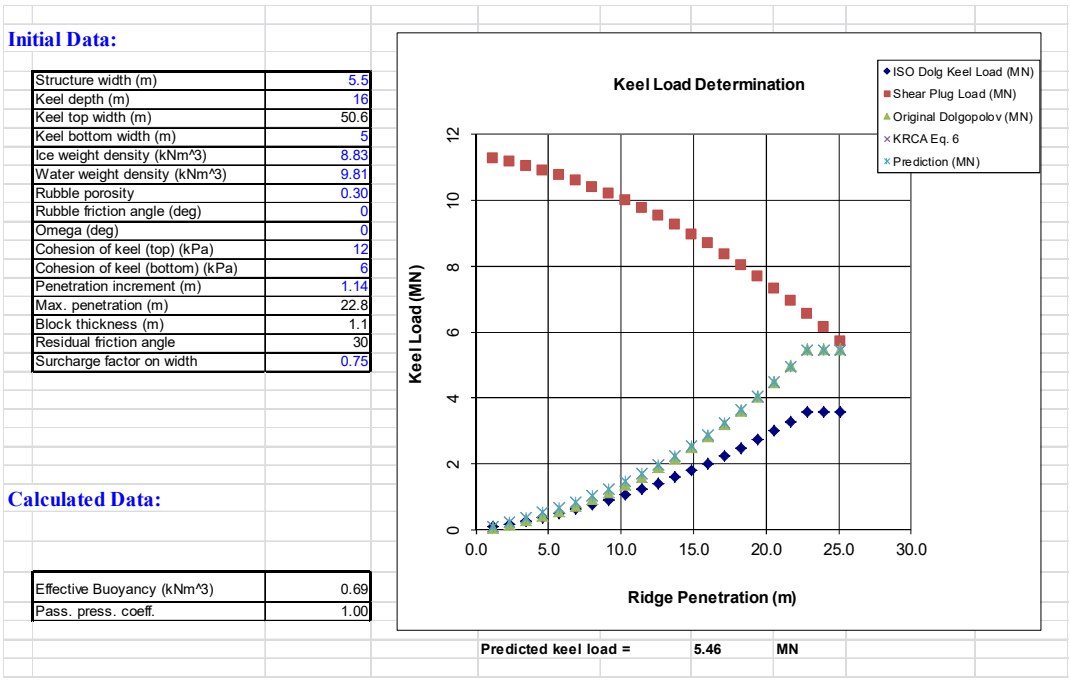

Fig. 11 - Keel load: downward breaking case with added surcharge to account for added debris from CL breaking

Comparison Up vs Down conical collars

A comparison of global loads for a 60 degree conical collar on a 5m dia. wind turbine shaft is shown in Table 5. For level ice there is a clear advantage with the down breaking configuration. For ridges, which are the controlling global design loads, there appears to be no significant difference (for the case shown). As expected the breaking term for the CL is higher but clearing forces which are accounted for by increasing the keel surcharge are lower.

Table 5: Ice load comparisons Up vs down breaking conical collars (60º) on a 5m dia. shaft (loads in MN)

Configuration	Level ice 0.6m		Ridge: CL = 1.1m; keel thickness = 16m			
		CL breaking	CL clearing	CL total	Keel load	Total ridge load
Up	1.34	1.4	1.9	3.3	4.58	7.9
Down	0.65	2.35	0 (added to keel as surcharge	2.35	5.46	7.8

Cyclic loads

As mentioned in the introduction, wind turbine bases are usually very sensitive to dynamic loads because of their slender nature. Parallel work was also carried out on ice load dynamic loading (Croasdale et al 2016b), but the topic is beyond the scope of this paper. It is sufficient to say that ridge loads controlling overall global load design will have a load signature dominated by the keel which rise and fall over several minutes and will not excite the structure. However, cyclic loads will be generated by the level ice and the CL of ridges. Schemes to develop ice load signatures and total number of cycles have been developed. Conical collars (up or down) help to get frequencies well away from the structure natural frequencies and hence dynamic excitation can be avoided.

Conclusions and recommendations

Methods for the calculation of ridge loads on typical wind turbine bases with conical collars have been reviewed and further developed. The gap in current methodologies was how to calculate the downward breaking of the consolidated layer of a ridge as it is pushed into the keel below. A method has been developed for this loading case and ice loads have been calculated for a typical design of wind turbine currently being planned for the US sector of Lake Erie.

For level ice there is a clear advantage with the down breaking configuration (for the case examined of 0.6m ice the load is reduced from 1.34 to 0.65MN. For ridges, which are the controlling global design loads, there appears to be no significant difference (for the case shown the ridge load is estimated to be 7.9MN for upward breaking and virtually the same for downward breaking (7.8MN)). As expected the breaking term for the CL is higher as it has to be pushed down into the keel, but clearing forces which are accounted for by increasing the keel surcharge are lower.

The uncertainties relating to ridge loads on downward breaking configurations are higher because there are no precedents yet built (subject to ridges). Whereas for upward breaking, there has been over 20 years of experience with Confederation Bridge in Canada which has an upward breaking conical collar on each of the piers. Experience at the Bridge giving typical ridge loads is included in a parallel paper at this conference (Croasdale et al 2018).

Further work to reduce uncertainties could include targeted physical test as well as numerical analysis methods using discrete element methods.

Acknowledgements

The authors thank ODE (London UK) for supporting this work (on behalf of LEEDCo) (Lake Erie Energy Development Company). They also thank Lorry Wagner of LEEDCo for encouragement and permission to publish at ATC.

References

Allyn N. and Croasdale, K. R., 2016. Ice Loads on Wind Turbine Foundations in Lake Erie – A Review. A report for LEEDCo Ice Breaker Project, Oct, 2016

Brown, T.G., Tibbo, S., Shrestha, N,. Tripathi, D, Obert, K., Bruce, J.R., Maes, M.A., 2010. Analysis of ice interactions and ice loads on Confederation Bridge. University of Calgary report to Strait Crossing.

Croasdale, K. R., 1980. Ice forces on fixed rigid structures. In Working Group on Ice Forces on Structures, IAHR. A State of the Art Report, CRREL Special report 80-26. Hanover, NH, USA.

Croasdale, K.R., Cammaert, A.B. and Metge, M.,1994. A method for the calculation of sheet ice loads on sloping structures. Proceedings of the 12th International Symposium on Ice of IAHR. Trondheim, August 1994 Norway (12 pages).

Croasdale, K. R.,2012. A Simple Model for First-year Ridge Loads on Sloping Structures. ICETECH, Banff, 2012.

Croasdale K.R., Brown T.G., Fuglem, M., Li, G., Shrestha, N., Spring, W., Thijssen J., Wong, C., 2016a. Improved equations for the actions of thick level ice on sloping platforms**.** ATC conference, St John's NFLD (October 2016) (OTC 27385).

Croasdale, K.R., Allyn, N., Thijssen, J., 2016b. Ice Load Signatures and Frequencies: Wind Turbine Foundations in Lake Erie. A report by K.R. Croasdale and Associates and CMO for LEEDCo Icebreaker Project. November 7, 2016

Croasdale K.R., Brown T.G., Li, G., Spring, W., 2018. First Year Ridge Interaction on Upward Sloping Structures: A New Approach. ATC Conference, Houston, 2018

DNV-OS-J101, 2014.Design of Offshore Wind Turbine Structures. May 2014. DNV-OS-J101.

Dolgopolov, Y.V, Afanasiev, V.P., Korenkov, V.A. And Panfilov, D.F., 1975. Effect of hummocked ice on the piers of marine hydraulic structures, Proc. 3rd Int. Symp. on Ice Problems, Hanover, USA, pp. 469-477.

IEC, 2009. Wind turbines - Part 3: Design requirements for offshore wind turbines. February 2009. IEC 61400-3.

ISO 19906 2010. International Standards Organisation. Petroleum and natural gas industries — Arctic offshore structures. ISO 19906:2010.

Karna, T. and Turunen, R.,1989. Dynamic response of narrow structures to ice loading. Cold Regions Science and Technology. Vol 17, 17: 173-187.

Palmer, A. C. and Croasdale K. R.,2013. Arctic Offshore Engineering. World Scientific Publishing Co. Ltd., Singapore. 2013.

Ralston, T.D.,1980. Plastic limit analysis of sheet ice loads on conical structures. Proceedings, IUTAM (International Union of Theoretical and Applied Mechanics) Symposium on physics and mechanics of ice, Copenhagen, pp. 289-308

Sudom, D., Timco, G., Sand, B. and Fransson L., 2011. Analysis of first - year and old ice ridge characteristics Proceedings, 21st International Conference on Port and Ocean Engineering under Arctic Conditions, Montréal.

Timco, G.W., Croasdale, K. R., Wright, B., 2000. An overview of first-year ridges. CHC Technical report HYD-TR-047. PERD CHC Report 5-112.Ottawa, 2000.